

# Simulation sensitivities of the major weather regimes of the Southeast Asia region

Chainarong Raktham · Cindy Bruyère · Jiemjai Kreasuwun · James Done · Chitrlada Thongbai · Wonchai Promnopas

Received: 17 October 2013 / Accepted: 17 April 2014 / Published online: 22 May 2014  
© The Author(s) 2014. This article is published with open access at Springerlink.com

**Abstract** This study evaluates the Weather Research and Forecasting model's ability to simulate major weather phenomena [dry conditions, tropical cyclones (TCs) and monsoonal flow] over East and Southeast Asia. Sensitivity tests comprising different cumulus (Kain–Fritsch and Betts–Miller–Janjic) and microphysics (Purdue Lin, WSM3, WSM6 and Thompson) are used together with different placement of lateral boundaries to understand and identify suitable model configuration for weather and climate simulations over the Asia region. All simulations are driven with reanalysis data and use a nominal grid spacing of 36 km, with 51 levels in the vertical. The dry season showed little sensitivity to any configuration choices, while the TC case shows high sensitivity to the cumulus scheme and low sensitivity to the microphysical scheme. Monsoon simulations displayed significant sensitivity to the placement of the lateral boundaries.

**Keywords** Model sensitivity · Tropical cyclone · WRF · Southeast Asia

## 1 Introduction

Tropical cyclones (TCs) are responsible for exchanging energy between oceans and the atmosphere and between the low and high latitudes, releasing enormous amounts of latent heat. TCs are also thought to play a large role in driving the global and regional water cycle by enhancing low-level convergence that supply the free troposphere with an upward flux of unstable air, which in turn brings moisture from the ocean to the land (Raymond 1995). In some cases, TCs can bring severe weather events like flashfloods, landslides, and storm surge.

Thailand in Southeast Asia is affected by TCs both directly and indirectly. In 2005, tropical storm Vicente made landfall on the Indochina peninsula from the South China Sea (SCS). Cabinet resolution (Thailand Cabinet resolution 2005) reports that the storm killed 4 people, injured several and severely affected more than 150,000. The storm affected 16 provinces throughout Thailand, washed away roads and bridges, closed schools, and caused severe damage to more than 100,000 acres of agricultural land. Vicente originated over the Northwest Pacific Ocean and moved westward across the Philippines before making landfall (Raktham et al. 2007). In 2004, Typhoon Chantu, also a Pacific storm with a westward track made landfall in Vietnam, and caused deadly flooding in Vietnam, Laos and Thailand and caused substantial changes in river levels (Wangwongchai et al. 2010). These westward tracking storms are recognized as causing high impacts in East and Southeast Asia (Harr and Elsberry 1991; Guo et al. 2012).

There is evidence that TCs are affected by climate change (Knutson et al. 2010). Webster et al. (2005) showed that over the last 30 years there has been a trend toward a larger proportion of the most intense TCs over most ocean basins including the Northwest Pacific. Holland and

---

C. Raktham (✉) · J. Kreasuwun · C. Thongbai · W. Promnopas  
Department of Physics and Materials Science, Faculty of  
Science, Chiang Mai University, Chiang Mai 50200, Thailand  
e-mail: glaraktham@gmail.com

C. Bruyère (✉) · J. Done  
National Center for Atmospheric Research, Boulder, CO, USA  
e-mail: bruyerec@ucar.edu

C. Bruyère  
Environmental Sciences and Management, North-West  
University, Potchefstroom, South Africa

Bruyère (2013) reported a strong link between the anthropogenic signal and the proportion of intense hurricanes that form in any given basin. Stowasser et al. (2007) indicates a continued trend towards higher proportion of the most intense TCs under future warming scenarios. Shibin and Bin (2013) found that the recent increase of TC numbers in the West North Pacific in May is the result of an enhanced summer monsoon over the South Asia and SCS.

In Taiwan, TCs alone contribute nearly 50 % of the total annual precipitation (Chen et al. 2010) so future changes in TC rainfall as suggested by Knutson et al. (2010) may have important consequences for the region (e.g., Chotamonsak et al. 2011). Indeed, a summary of six modeling studies reported model consensus of a future increase in rainfall rates over the Northwest Pacific basin (Ying et al. 2012).

Thailand is also influenced by the Southwesterly monsoon, a subcomponent in the East Asian Summer Monsoon (EASM) (Tao and Chen 1987). The EASM, in turn, sometimes interacts with Indian Summer Monsoon, which can lead to anomalies in the monsoonal rainfall patterns over this area (Wei et al. 2013). As defined by Ramage (1971), EASM starts to flow through South East Asia during early May and affects Thailand from mid May (Wang and Lin 2002). Monthly precipitation over the Thailand region is significantly enhanced during the monsoon season (May through October; Ding and Chan 2005).

Due to the large impact TCs and the EASM have on the East and Southeast Asia region, it is important to study their potential changes under future climate change projections in order to understand the possible impact these changes will impose in terms of precipitation, especially heavy precipitation and flood events. The Weather Research and Forecasting (WRF) model (Skamarock et al. 2008) is a flexible and powerful tool to simulate and understand TC and monsoon climatology, specifically since this limited area model enables far higher resolution simulation over a region of interest than is possible using a global climate model. The WRF model has already been used successfully to study TC activity under climate change scenarios (Done et al. 2012, 2013). Regional climate simulations can be very sensitive to aspects of model setup such as domain size and model physics and this sensitivity can vary by geographic region and season (Rosenthal 1971; Solomon et al. 2007; Gentry and Lackmann 2010). It is therefore critical to understand sensitivities of the modeling system for simulation of TCs and EASM prior to embarking on a climate change study.

In this paper, we explore the sensitivity of WRF (version 3.3.1) model simulations in East and Southeast Asia to aspects of model design and understand the importance of domain size and model physics parameterizations. In Sect. 2, we present the experimental design. Section 3 presents

results of the sensitivity studies and we conclude the paper with a discussion in Sect. 4.

## 2 Data and experimental design

### 2.1 Data

The driving data for the WRF model is the National Centers for Environmental Prediction (NCEP)/National Center for Atmospheric Research (NCAR) Reanalysis Project (NNRP) data (Kalnay et al. 1996) available 6 hourly at 00, 06, 12 and 18UTC since 1948 on a global  $2.5^\circ \times 2.5^\circ$  grid. Rather than using sea surface temperature (SST) data from NNRP, the Reynolds optimum interpolated (OIv2) SST analyses (Reynolds 1988; Reynolds and Marsico 1993) are used. These data are at a temporal resolution of a week and on a horizontal grid of  $1^\circ \times 1^\circ$ , provided by the National Oceanic and Atmospheric Administration (NOAA), US.

Tropical Rainfall Measuring Mission data (TRMM; Huffman et al. 2007), provided by the Goddard Distributed Active Archive Center, and rain gauge data provided by the Thai Meteorological Department are used to compare the ability of WRF to capture the observed precipitation patterns. TRMM data are available daily on a  $0.25^\circ \times 0.25^\circ$  grid.

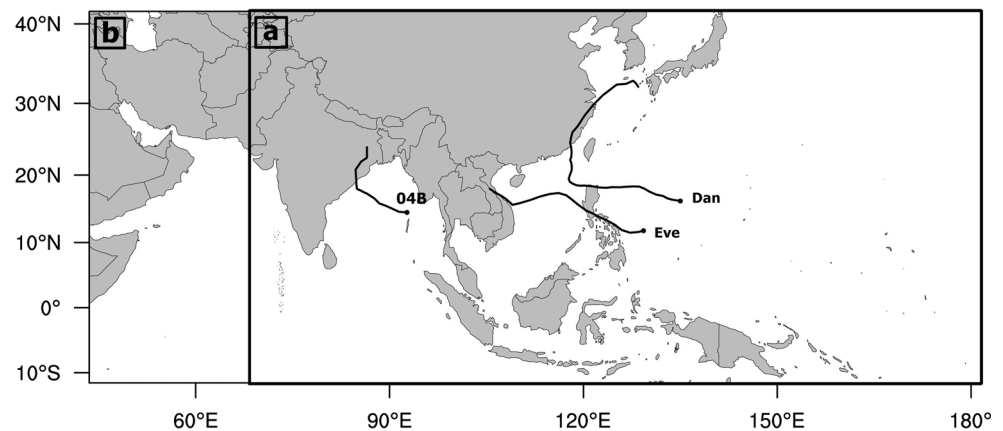
Tropical cyclone observations are taken from the International Best Track Archive for Climate Stewardship (IBTrACS; Knapp et al. 2010). IBTrACS is the official dataset for TC best track data (provided by NOAA), and contains globally consistent 6-hourly TC information including location and intensity.

### 2.2 Experimental design

In this study, we examine simulation sensitivity to moist physical parameterizations in terms of two major East and Southeast Asia weather phenomena, namely (1) TC genesis and lifecycle, and (2) EASM. Monsoons and TC activity are closely tied to deep moist convection and therefore likely to be particularly sensitive to details of the cumulus parameterization such as threshold triggers, and to microphysics through the fall speed representation and radiation effects. The partitioning of latent heat release between cumulus and microphysics schemes and vertical distribution is also likely to be critical.

The cumulus parameterization schemes evaluated are the Kain–Fritsch (KF) scheme (a cloud model mass flux scheme that includes entrainment and detrainment; Kain 2004) and the Betts–Miller–Janjic (BMJ) scheme (a sounding adjustment scheme without cloud detrainment; Janjic 2000). For microphysical processes, we evaluated four schemes: (1) The Purdue Lin scheme (Lin et al. 1983), a 5-class scheme

**Fig. 1** Domains used in the sensitivity experiments. The smaller domain **a** was used in all the model experiments, while the larger **b** domain was only used for select model runs. The *track lines* indicate the observed Tropical Cyclones for October 1999: Typhoons Dan (October 1–11) and Eve (October 14–20), and Cyclone 04B (October 15–19)



that allows mixed phase; (2) The WRF single-moment 3-class scheme (WSM3; Hong et al. 2004), a simple ice scheme with vapor, cloud water/ice and rain/snow which does not allow mixed phase; (3) The WRF single-moment 6-class scheme (WSM6; Hong and Lim 2006), a 6-class scheme with combined snow/graupel fall speed estimation; and (4) The Thompson scheme (Thompson et al. 2004), a 6-class microphysical scheme that allows mixed phase and also predicts ice and rain number concentrations. These schemes were selected based on available schemes in the version of the model that we used (version 3.3.1) that were appropriate for the resolution of our model simulations.

In this study, we used a domain configuration (domain a shown in Fig. 1) that covers the area 12S to 42N and 70E to approximately 180E. This area includes both the North–West Pacific and the North Indian Oceans. This geographical area is sufficiently large to capture TC genesis, tracks and TC-related precipitation, as well as monsoon development. The domain uses a horizontal grid spacing of 36 km, with 51 levels in the vertical, up to a height of 10 mb. A larger domain (domain b in Fig. 1), extending to 43E was also used for select model runs.

Readily available rain gauge data are limited to within Thailand and cannot provide data for neighboring countries or precipitation over the oceans. Here we examine the quality of TRMM data over Thailand to determine its suitability over the wider region. Figure 2 shows the 24-h precipitation accumulation on October 15, 1999 from TRMM and observation station data across Thailand. Precipitation patterns over Thailand for TRMM data closely match those for surface station observations. Nine observational stations (*Bangkok, Chiang Mai, Phitsanulok, Ubon Ratchathani, Nakhon Ratchasima, Songkhla, Narathiwat, Prachuap Khiri Khan, and Phuket*) were selected to calculate the average monthly rainfall. Figure 3 shows good agreement between these rain gauge monthly-accumulated precipitation averages for the year 1999, and the TRMM data for these stations. In summary, TRMM data

are good estimates for surface observed precipitation. Therefore only TRMM data are used as a comparison to WRF model output.

Weather in Thailand is strongly affected by the East Asian Summer Monsoon. March (Fig. 3) recorded the lowest rainfall amounts, while May and October recorded the highest amounts. This bimodal distribution in the annual precipitation patterns for this region is due to the Southwestern monsoon that starts in May as the monsoonal trough shifts northwards over China and the return of the monsoonal trough in October.

Tropical storms in the Northern West Pacific (99E–182E) and Bay of Bengal (80E–99E and 0N–42 N) can occur throughout the year, although the latter half of the year is the active TC season. Since we want to study rainfall in Thailand, and WRF’s ability to correctly simulate precipitation events, we selected (1) a month that has both high rainfall and has been influenced by TCs (October, during which 3 storms developed (Fig. 1); a westward tracking Pacific storm, a recurving Pacific storm, and a Bay of Bengal storm.), (2) a month with high precipitation amounts, but associated with monsoon activity rather than TC related precipitation (May recorded 2 TCs; the first dissipating around May 3, and the second only developed on May 30, leaving May essentially TC free), and (3) a contrasting dry month, with no TC activity (March, Fig. 3). Finally, the specific dates for analysis have been determined as: (1) Dry case: March 1–17, 1999; (2) TC case: October 5–21, 1999; and (3) Monsoon case: May 15–24, 1999. To allow the model to fully spin-up convection the first 2 days in each case are considered as the spin up period (Falk et al. 2013) and ignored for the purposes of analysis.

### 3 Sensitivity experiments

The aim of the sensitivity experiments is to understand the aspects of the WRF model setup that are important to

**Fig. 2** The 24-h precipitation accumulation (mm) on October 15, 1999 in TRMM data (left) and station observations across Thailand (right)

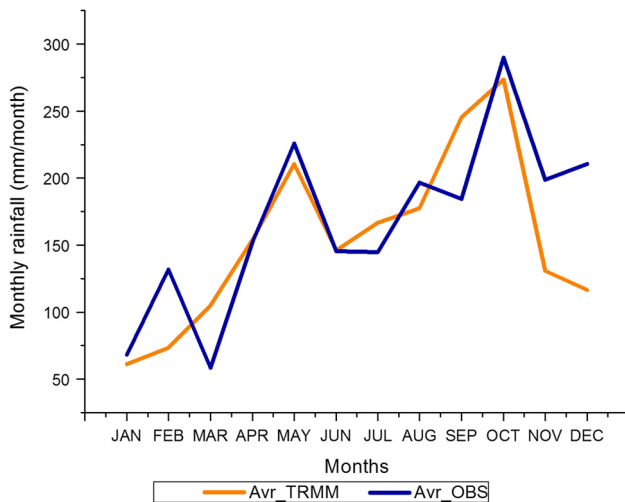
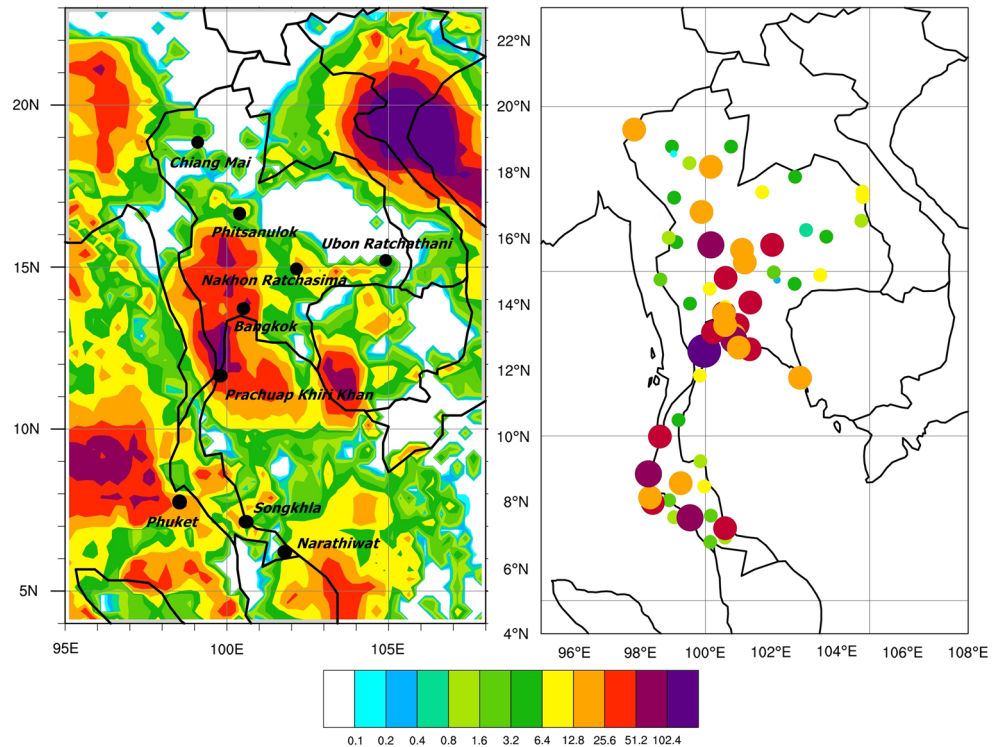


**Fig. 3** Average monthly precipitation (mm) over Thailand for the year 1999, from station observations (blue line) and TRMM (orange line)

capture the major weather phenomena in the East Asia region. To this aim, we evaluate the sensitivity of the WRF model to moist physics parameterization options under dry, TC, and monsoon conditions.

### 3.1 Dry case

For the dry case, the model is run for the 2 weeks, March 1–17, 1999. Figure 4 shows the NNRP 850 hPa wind and

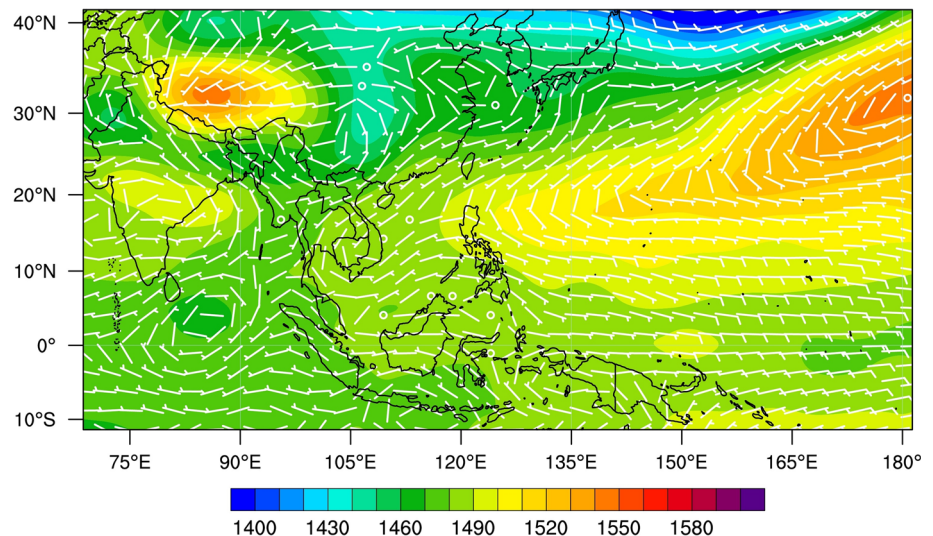
geopotential height composite fields for the period March 3–17, 1999. This shows that the eastern half of the area is dominated by a high-pressure system, with associated anti-cyclonic flow. Some anti-cyclonic disturbances are present over the western half of the domain, while a southwesterly wind is influencing most of Thailand.

Figure 5 shows the 850 hPa wind and geopotential height difference fields (WRF–NNRP) averaged for the period March 3–17, 1999 for the four microphysics parameterizations (Lin, WSM3, WSM6 and Thompson) and two cumulus parameterizations (KF and BMJ). The difference fields are very similar across all simulations and show that WRF slightly underestimates the high-pressure system over the east, and overestimates the pressure in the southern half of the domain. This difference in the southern half of the domain is worse for all the BMJ cases compared to KF. Winds and geopotential heights in the model simulations are more sensitive to the cumulus parameterization than the microphysics parameterization.

The TRMM precipitation for this period (*not shown*), is mostly light and confined to the oceans, with dry areas over land. The heaviest precipitation is around the equator and to the north, east of China. The WRF simulated precipitation for all eight simulations captures the major spatial precipitation patterns, although all the simulations overestimated the amount of precipitation. The BMJ simulations compare slightly better to TRMM (Fig. 6e–h), producing less precipitation than the KF simulations (Fig. 6a–d), although even these over-estimated the precipitation



**Fig. 4** Average NNRP850 hPa wind (*wind barbs*) and geopotential height (*colors, m*) for the period March 3–17, 1999



amounts. BMJ systematically overestimated the average domain wide precipitation for this period by 10 percent. KF overestimated the precipitation by 50 %, with the bulk of this over-prediction developing along the equator. Similar overestimations are observed by others (e.g., Liang et al. 2004). Since the patterns are similar to TRMM, corrected precipitation predictions can still be inferred from the model data through post-processing bias correction methods (e.g., PaiMazumder and Done 2013). As observed for the winds and geopotential heights, precipitation differences are bigger between different cumulus schemes than between different microphysical schemes.

In summary, for the dry case, all parameterizations performed similarly in terms of average low level flow and total precipitation, with model simulations closer to each other than any simulation is to the observations. The largest sensitivity is to the cumulus parameterization rather than the microphysics parameterization.

### 3.2 Tropical cyclone case

Figure 1 shows the observed TC tracks for October 1999 from IBTrACS (Knapp et al. 2010). Three TCs developed during our simulation period. TCs Dan and Eve were located in the Pacific Ocean, while TC 04B was an Indian Ocean TC. Typhoons Dan (October 1–11) and Eve (October 14–20) both developed over the Philippine Sea and made landfall in the Philippines and China, with Dan taking a more northerly route. Dan was a more intense storm, with a peak wind speed of 125 mph, causing multiple fatalities in the Philippines, while Eve's impact extended to central Vietnam. Cyclone 04B (October 15–19), with a peak intensity of 140 mph, resulted in more than 80 fatalities in the Orissa region of India.

Tracking tropical storms in model simulations requires the identification of TC like structures that satisfy a strict

set of criteria. In this paper we adopted the Suzuki-Parker (2012) automated tracking algorithm. This algorithm first identifies possible storms by finding local pressure minima. Non-TC like systems are filtered out using wind speed, vorticity, warm-core, duration, structure, and cyclone phase criteria as defined in Hart (2003).

Figure 7 shows all (blue and red tracks) local pressure minima initially identified as possible tropical storms in the WRF model simulations. The red tracks were later filtered out, while the blue tracks were defined by the Suzuki-Parker (2012) tracking algorithm as TCs. This raises questions as to the tuning required for the tracker when running the model at a grid spacing of 36 km, but for the purpose of this study, we will simply consider all possible storms, while paying special attention to the storms finally identified by the Suzuki-Parker algorithm.

For TC Eve (the westward tracking storm), only KF combined with three out of the four the microphysical schemes (Lin, WSM3, and WSM6, Fig. 7a–c) developed a westward propagating storm, although in all three cases this TC was so weak it was filtered out by the tracker. For TC Dan (the re-curving storm), although all the simulations developed a storm that first tracked westward before re-curving, only simulations using KF developed this storm into a strong enough system for the tracker to identify. In all simulations using BMJ, this disturbance failed to develop into a TC. All the simulations (excluding KF-WSM3), also developed a storm to the east of TC Dan, and most of the simulations developed this storm into a TC (excluding the KF-Thompson simulation), although a TC did not develop there in reality. This might be due to the lack of feedback in the simulation from the atmosphere to the ocean meaning the lack of a cold wake from TC Dan would result in a warmer ocean than in reality and provided a more favorable environment for storm development. This warm sea surface may also have encouraged the TC to



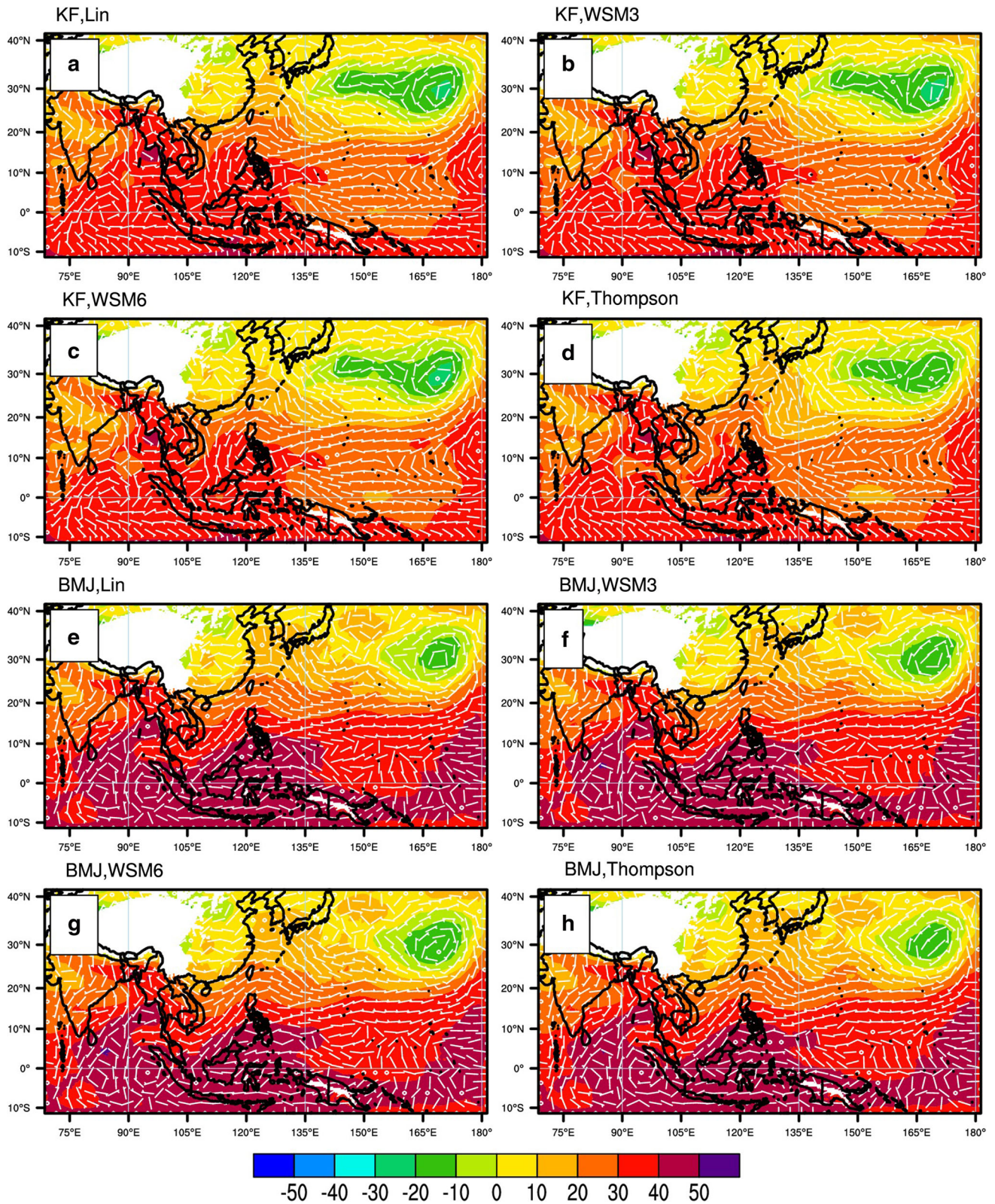


**Fig. 5** Average 850 hPa wind field (wind barbs) and geopotential height (colors, m) differences (WRF–NNRP) for the period March 3–17, 1999 using four different microphysical schemes (*Lin*, *WSM3*, *WSM6* and *Thompson*) and two cumulus schemes KF (a–d) and BMJ (e–h)



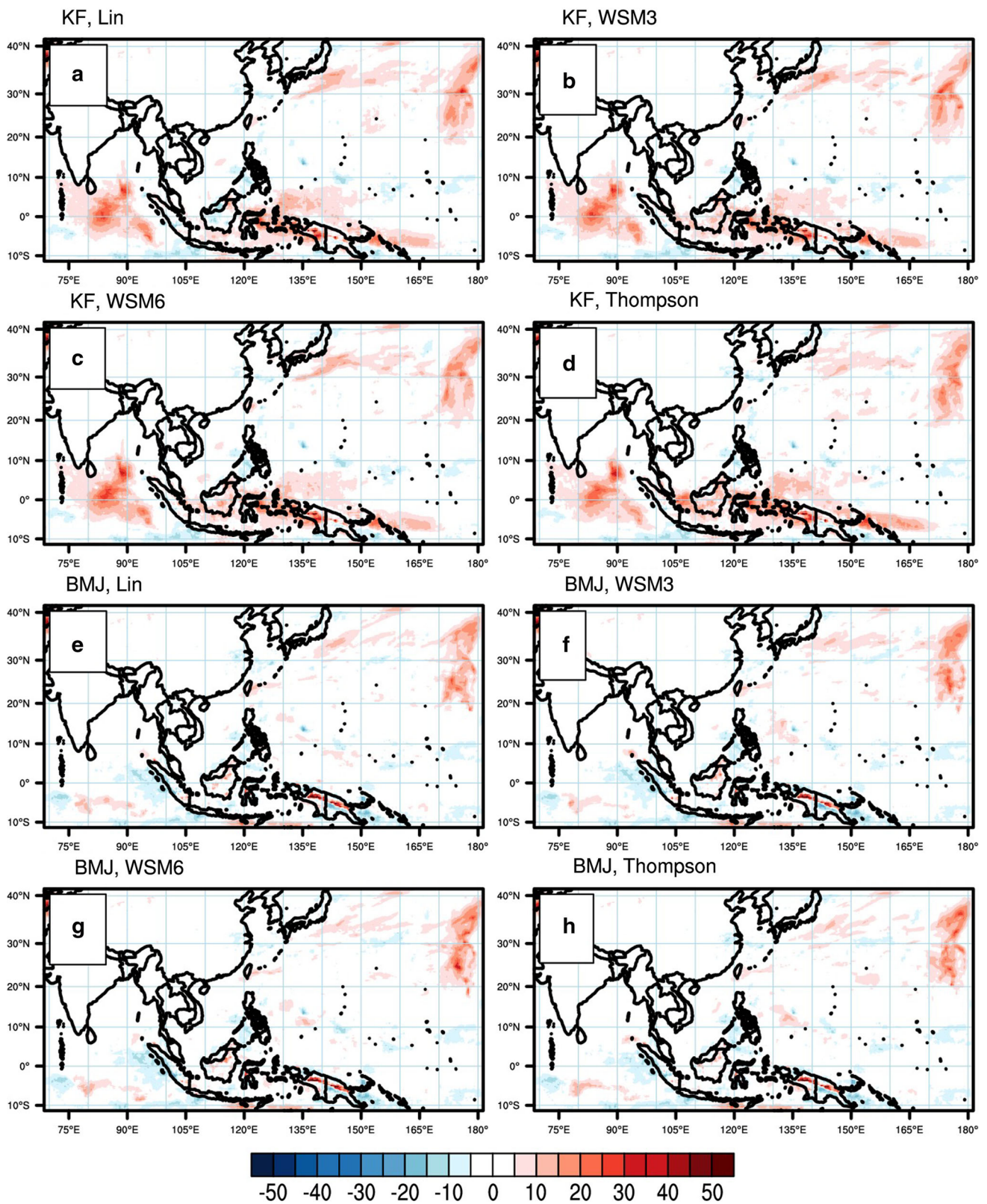


**Fig. 6** Precipitation (mm) differences between WRF and TRMM for the period March 3–17, 1999 using four different microphysical schemes (*Lin*, *WSM3*, *WSM6* and *Thompson*) and two cumulus schemes KF (a–d) and BMJ (e–h)

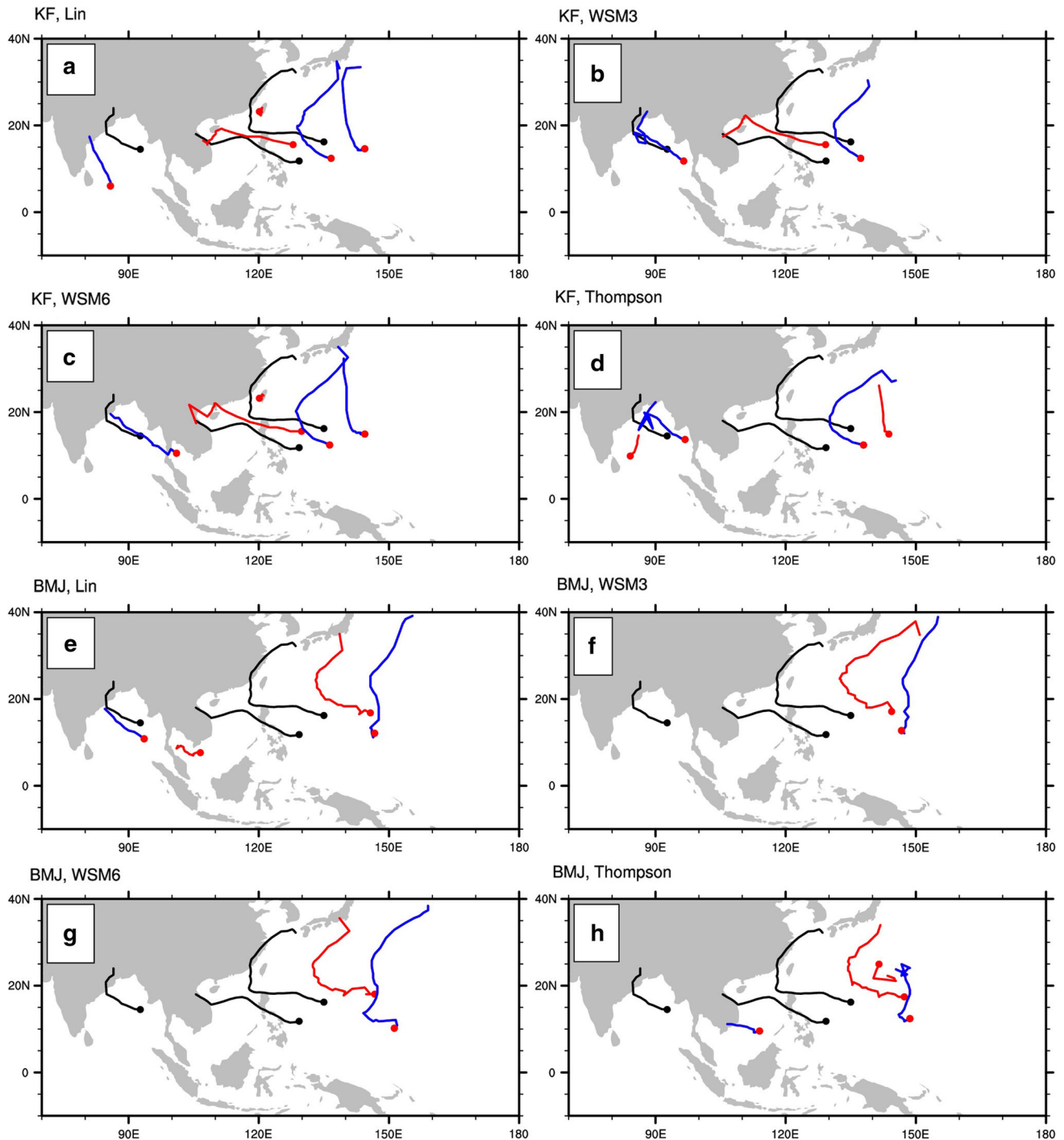


**Fig. 7** TC tracks developed by the WRF model for the four different microphysical schemes (*Lin*, *WSM3*, *WSM6* and *Thompson*) and two cumulus schemes KF (a–d) and BMJ (e–h). Shown are all possible

tracks (*blue* and *red*) developed by the model, while the blue tracks signify tropical cyclones as defined by the Suzuki-Parker (2012) tracker. The *black lines* indicate the observed storm tracks

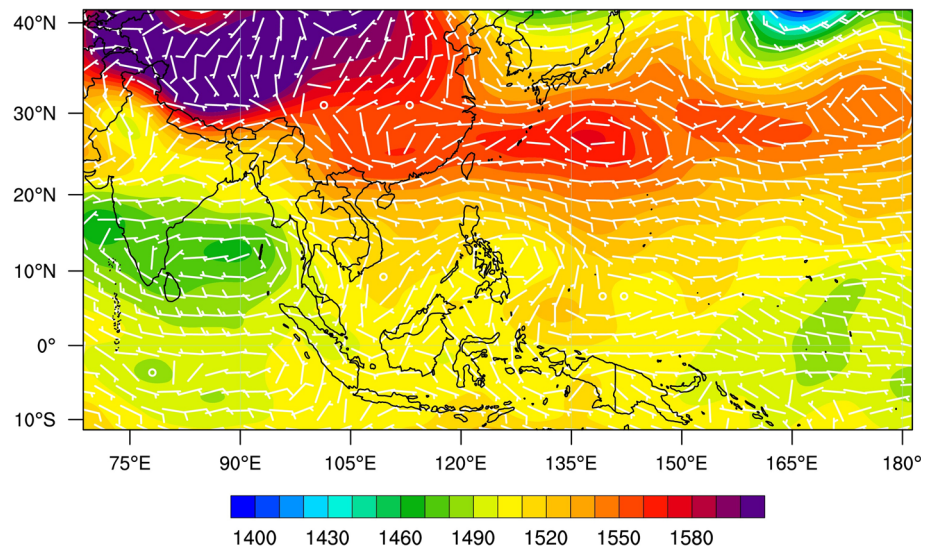
move eastward as reported by Yun et al. (2012). However, as this is a research topic in its own right, and not the focus of this study, we simply acknowledge but do not explore the possible deficiency in the model configuration. All KF simulations developed a TC in the Bay of Bengal, but only one BMJ (with *Lin*) simulation developed a TC in this

region. In summary, in terms of TC development, KF simulations fare better than BMJ simulations, with *Lin*, *WSM3* and *WSM6* performing the best for this case.

To better understand the differences in TC simulation, it is instructive to examine the large-scale environment. In this case the simulations are dominated by the developed



**Fig. 8** NNRP 850 hPa wind (wind barbs) and geopotential height (colors, m) on October 15, 1999



tropical storms, which precludes a quantitative analysis of the composites. We therefore only examine the large-scale flow by concentrating on a single simulation day. Here we arbitrarily picked October 15, 1999. Figure 8, the NNRP 850 hPa wind field and geopotential height for October 15, 1999, shows an easterly flow across all of Thailand and surrounding countries and a cyclonic flow near the Philippines, which is the initial stage of TC Eve. There is also a cyclonic flow present in the Bay of Bengal related to Cyclone 04B. A high-pressure system is situated over China and the East China Sea.

The simulated fields for October 15, 1999 (Fig. 9) using different physics parameterization choices show that KF simulations (a–d) all developed well-defined cyclone systems, while the BMJ simulations (e–h) developed extremely large, weak systems. On average, the maximum wind speeds for TCs in the KF simulations were 30 percent stronger than those in the BMJ simulations and the radius of maximum winds was 50 % larger for BMJ storms compared to KF storms. The KF simulations all correctly simulated the high-pressure system over China and the East China Sea, with the well-developed TC structures to the south as observed. The large TC structure in the BMJ simulations resulted in a breakup of the high-pressure system to the north, which led to a very different flow pattern over the Pacific Ocean. These findings, i.e., large, but weaker TC systems and incorrect weather patterns over the Pacific remain problems using the BMJ scheme throughout the simulation (*not shown*), with the KF simulations always outperforming the BMJ simulations. Differences due to microphysics schemes are far less than due to cumulus schemes, with WSM6 storms on average the strongest among the four simulations, while Thompson produced the weakest storms.

In terms of rainfall, the model over-predicted the total precipitation (*domain average and for the duration of the simulation*) amounts for all eight simulations, with KF producing more (30 % more than TRMM) precipitation than BMJ (10 % more than TRMM). The most apparent precipitation differences are along the TC tracks. When comparing TRMM data with the WRF model precipitation (Fig. 10), one can clearly see the passage of the model-developed TCs. The precipitation swaths also clearly show the difference between the cyclones developed by KF and BMJ with BMJ developing broader and more variable rain swaths than KF.

### 3.3 Monsoon case

The Monsoon case was run for the period May 15–24, 1999, again discounting the first 2 days as a spin-up period. For this case, we elected to eliminate some of the sensitivity studies based on past performance. For the dry case, the runs were more similar to each other than to the observations. On the other hand, the KF clearly outperformed the BMJ scheme in simulating TCs. Although only a single case, the BMJ's poor performance in simulating TCs prompted us to eliminate it from further sensitivity runs. All the microphysical schemes performed similarly, yet a number of other studies (Kim and Wang 2011; Ma et al. 2012; Shan et al. 2012) found that the Lin scheme performed well in the Asia region.

Thus, rather than running a physics ensemble for this case, we select the best performing physics from the TC case, and investigate the model's ability to (1) also capture monsoonal flow with the chosen physical option, and (2) test the model's sensitivity to the placement of the lateral boundaries. We therefore run the model with KF-Lin and KF-WSM3



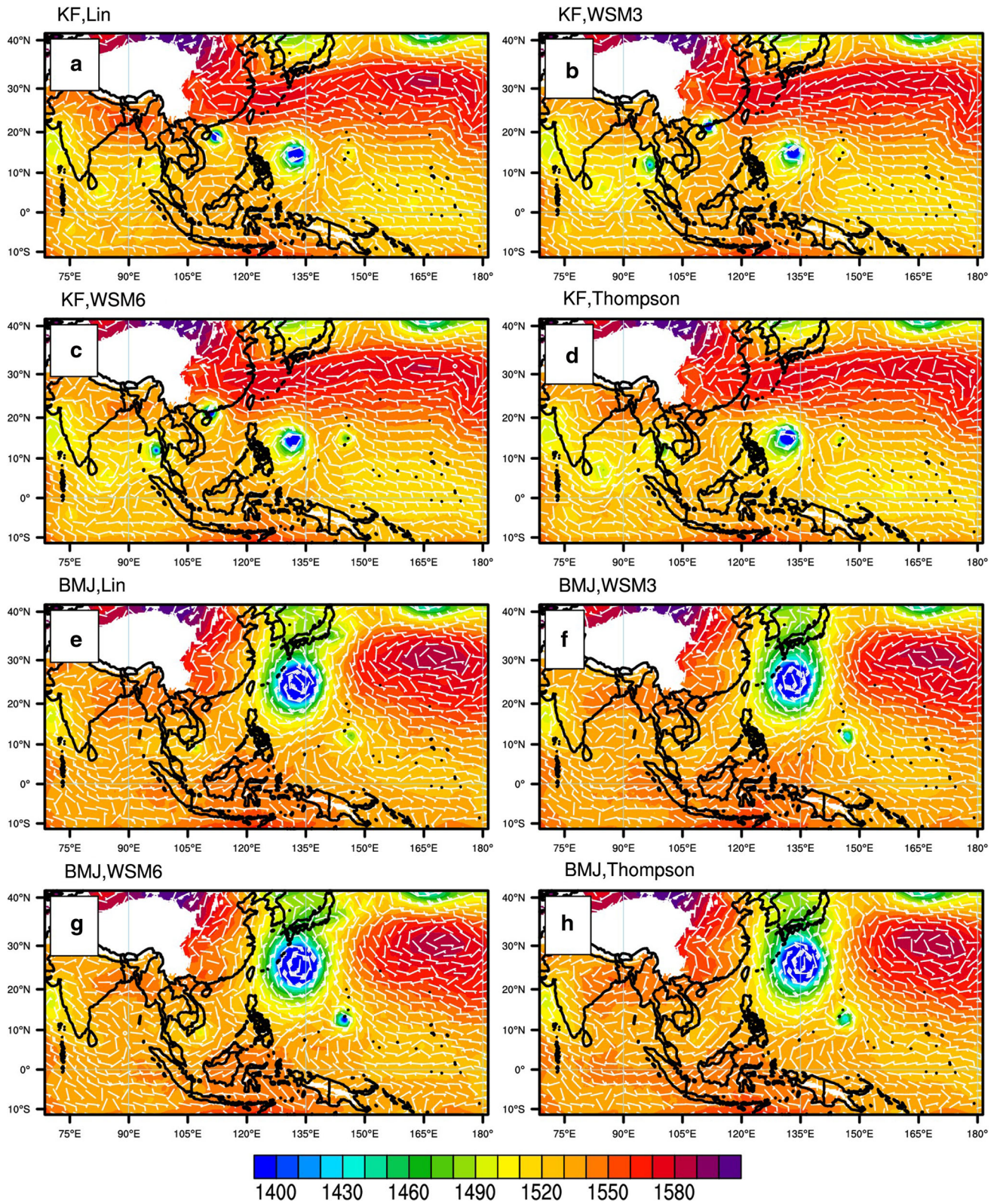


**Fig. 9** 850 hPa wind (wind barsbs) and geopotential height (colors, m) on October 15, 1999 from WRF using four different microphysical scheme (Lin, WSM3, WSM6 and Thompson) and two cumulus schemes KF (a–d) and BMJ (e–h)



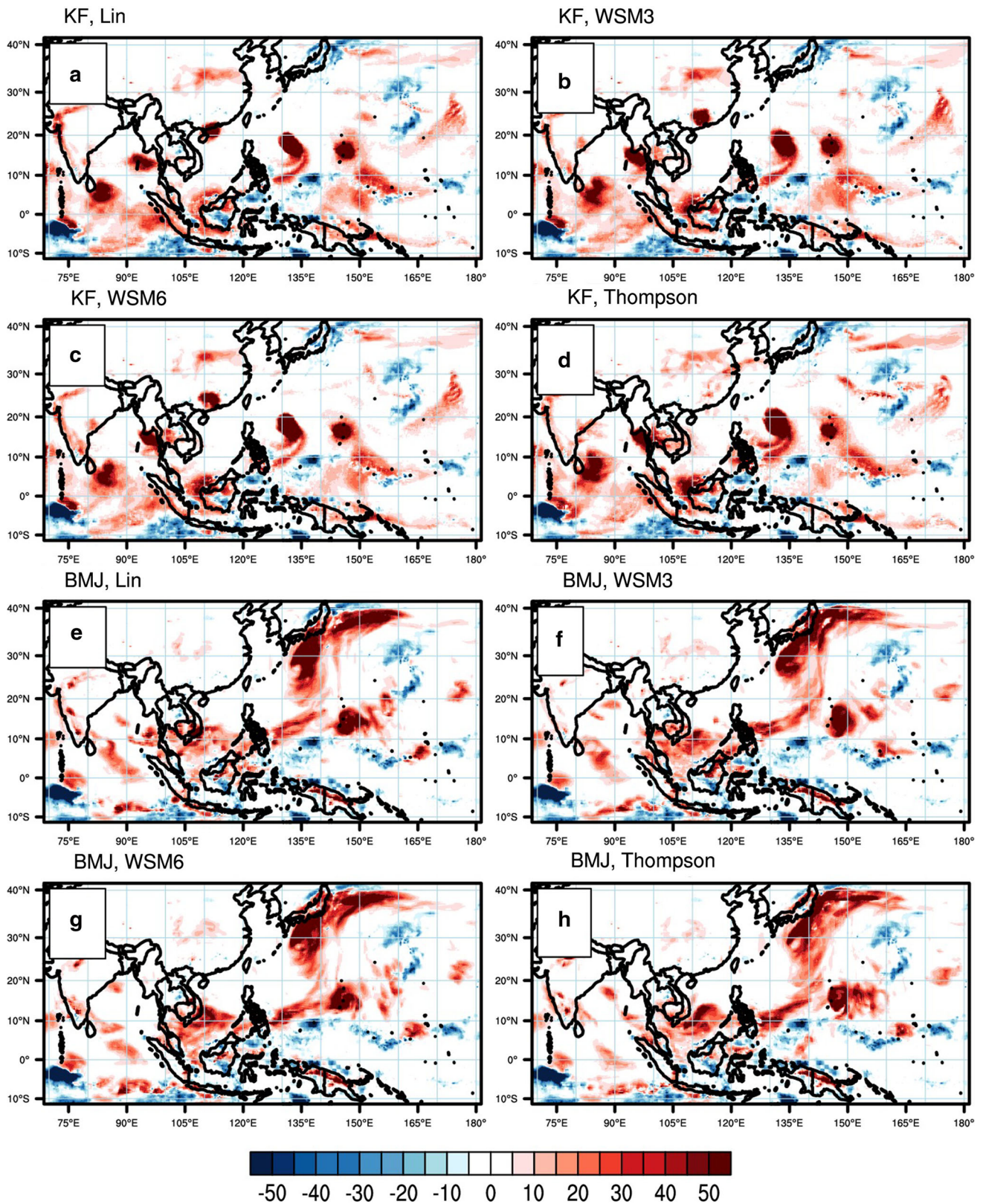
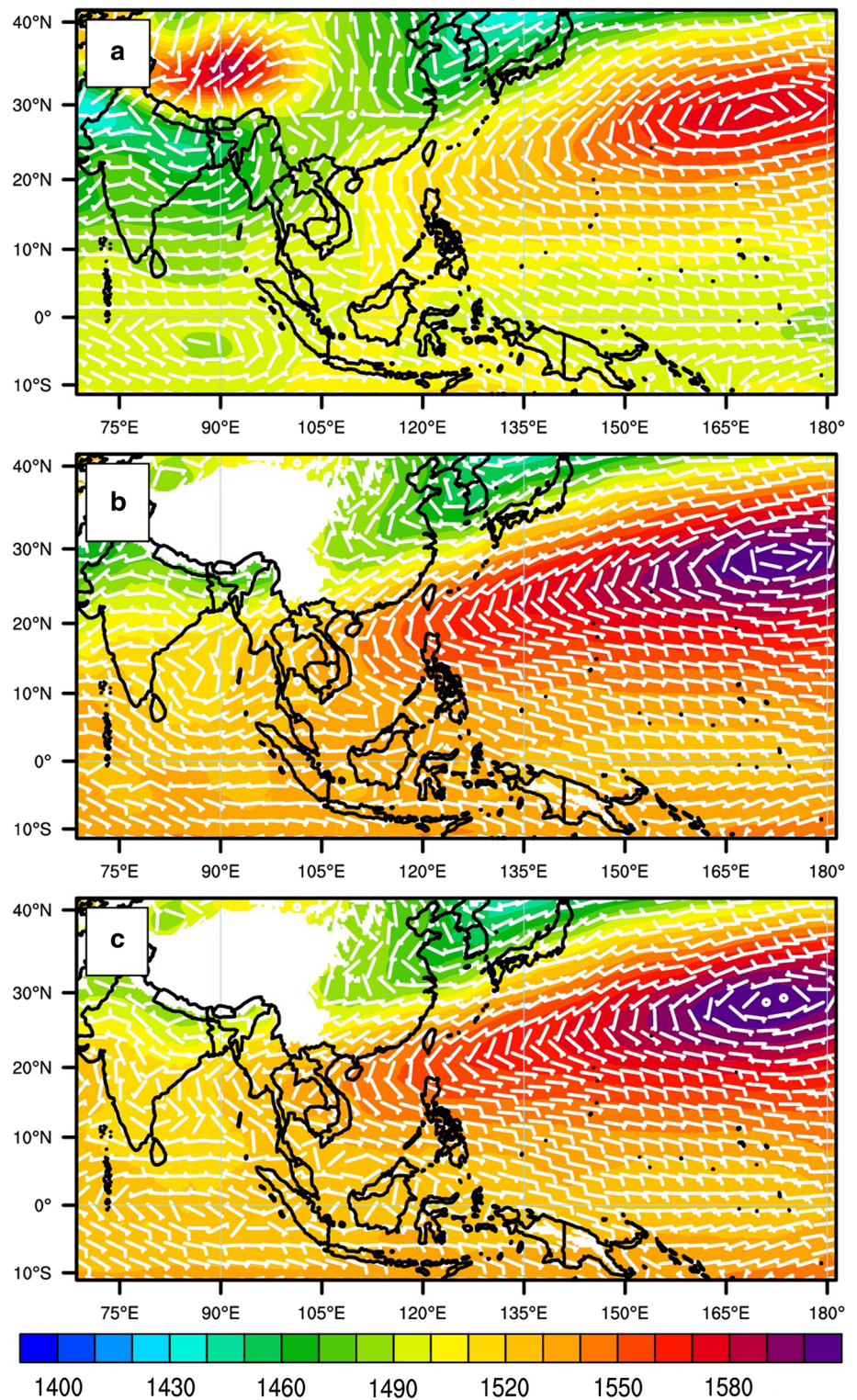


**Fig. 10** Precipitation (mm) differences between WRF and TRMM for the period October 7–21, 1999 using four different microphysical scheme (*Lin*, *WSM3*, *WSM6* and *Thompson*) and two cumulus schemes KF (a–d) and BMJ (e–h)



**Fig. 11** 850 hPa wind and geopotential height (m) averages for the period May 17–24, 1999 for **a** NNRP data, **b** the WRF model, and **c** the WRF model run on a bigger domain. For easier comparison, all data are shown on the smaller of the two domains

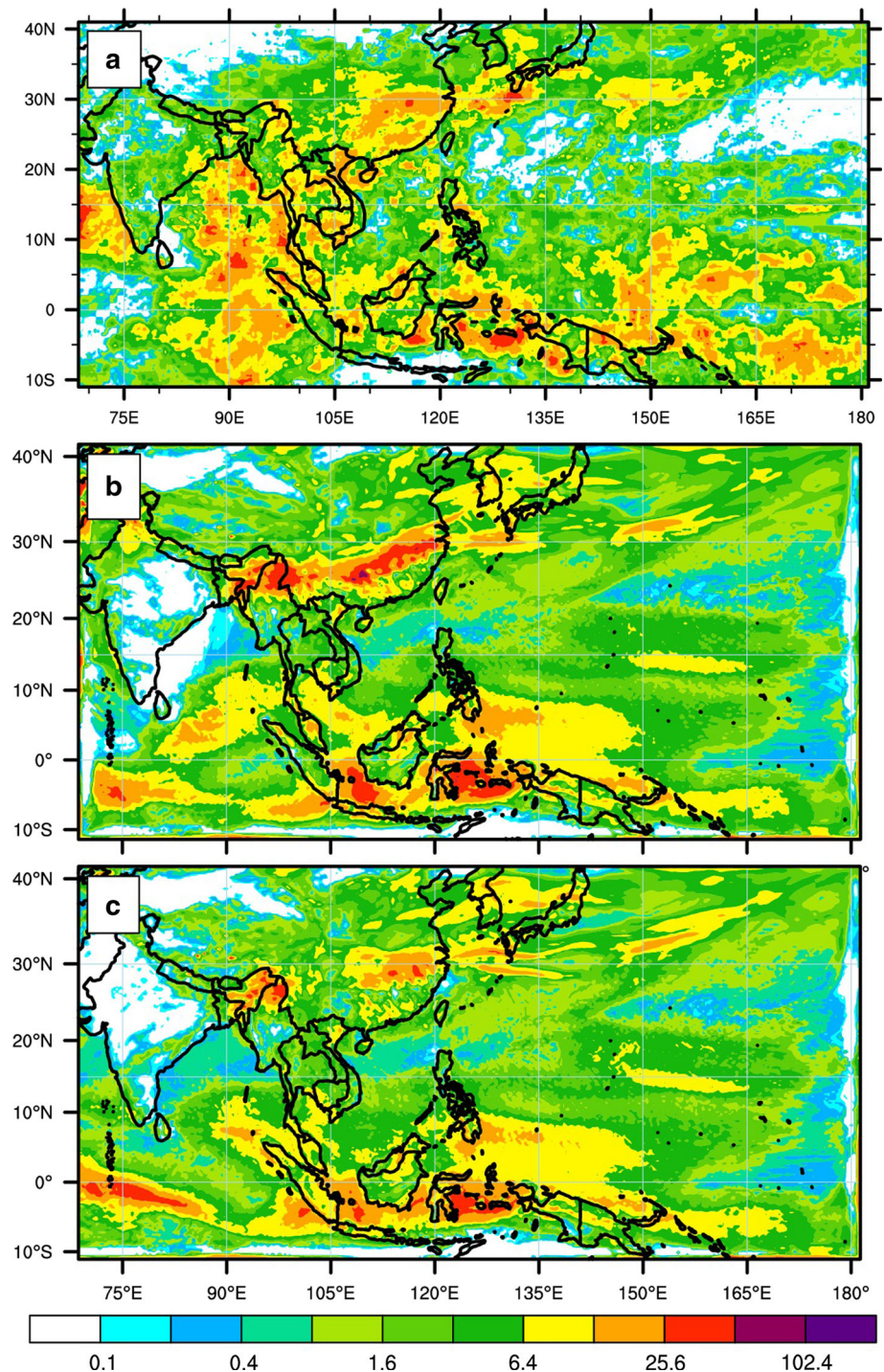


schemes, but on both the original domain (domain a in Fig. 1) and a larger domain that extends farther west (domain b in Fig. 1). As in the TC case, here the KF-Lin and KF-WSM3 configurations both performed similarly; therefore we only show results from the KF-Lin configuration.

Flow patterns under monsoon conditions are similar to those seen in the dry season, except that the southwesterly wind is stronger and more persistent, while the wind over India shifts more northerly. This brings moisture from the ocean overland, resulting in higher precipitation amounts.



**Fig. 12** Average precipitation for the period May 17–24, 1999, for **a** TRMM, **b** the WRF model, and **c** the WRF model run on a bigger domain. For easier comparison, all data are shown on the smaller of the two domains



The two model simulations develop similar height patterns to the NNRP height pattern (Fig. 11). The model wind patterns are also similar to those for NNRP. Monsoonal flow over India, Thailand and China is represented reasonably well in the simulation run on the smaller of the two domains (Fig. 11b). In the larger of the two domains (Fig. 11c) this monsoonal flow breaks down completely, suggesting a strong sensitivity to the placement of the inflow boundary.

May precipitation typically falls in a northeasterly belt over the Indian Ocean, Thailand and China, with a second belt of precipitation along the equator as shown in Fig. 12a. Both model simulations captured the precipitation belt along the equator, while both showed an incorrect break in the northeasterly precipitation belt (Fig. 12b, c). The run with the smaller domain simulated the northeasterly belt better, although there was a break in the rainfall pattern over the northern Thailand (Fig. 12b). For the larger

domain, the northeasterly belt was far weaker, resulting from the breakdown on the monsoonal flow over this area.

#### 4 Discussion

Southeast Asia experiences a variety of weather regimes including dry seasons, TC seasons and monsoonal flow. This study explores the ability of the WRF model using different representations of moist physics to capture these key weather regimes. Through short period simulations an understanding of the model performance has been developed and establishes the model as a suitable tool for future work on regional climate predictions over this area. Specifically, we selected a dry period, a TC period, and a monsoon period, and examined the performance of eight combinations of cumulus and microphysical parameterization schemes.

All combinations are able to capture the basic flow patterns observed during the dry season, and the WRF model shows no sensitivity to parameterization options under these conditions. For the TC case, all simulations using BMJ cumulus parameterization created unrealistically large and weak tropical storms. This resulted in subsequent anomalous atmospheric flow patterns compared to observations. Simulations using the KF scheme generated realistic looking TCs and reasonable atmospheric flow patterns with only small sensitivity to the microphysics parameterization, with the WSM6 scheme generating the strongest storms, and the Thompson scheme the weakest storms. Lin and WSM3 performed similarly in these runs, although other papers reported improvements when using the Lin scheme. This low sensitivity of TC simulation to microphysics is similar to the results of Tao et al. (2011).

For the dry and TC cases, the WRF model consistently developed reasonable precipitation patterns, although precipitation amounts were always over-estimated. For the monsoon case, the physics combination that created the best TC simulations (KF-Lin and KF-WSM3) also performed satisfactorily. However, when the domain inflow boundary was moved farther west, the monsoonal flow broke down completely, which also resulted in an incorrect precipitation pattern, suggesting that the monsoon flow is highly sensitive to the placement of the inflow boundary and/or domain size.

In summary, this study has identified a WRF model configuration that is able to correctly simulate most atmospheric regimes over Southeast Asia, albeit with overestimation of precipitation. Future work will utilize this model configuration to simulate longer time periods to improve our understanding of potential future changes to the dominant weather regimes over Southeast Asia.

**Acknowledgments** This study was financially supported by the Development and Promotion in Science and Technology (DPST) of the Thai government and received expert advice from the Regional Climate Section, National Center for Atmospheric Research (NCAR), USA.

**Open Access** This article is distributed under the terms of the Creative Commons Attribution License which permits any use, distribution, and reproduction in any medium, provided the original author(s) and the source are credited.

#### References

- Chen J-M, Li T, Shih C-F (2010) Tropical cyclone and monsoon-induced rainfall variability in Taiwan. *J Clim* 23:4107–4120
- Chotamonsak C, Salathe EP, Kreasuwan J, Chantara S, Siriwitayakorn S (2011) Projected climate change over Southeast Asia simulated using a WRF regional climate model. *Atmos Sci Lett* 12(2):213–219
- Ding Y, Chan JCL (2005) The East Asian summer monsoon: an overview. *Meteorol Atmos Phys* 89:117–142
- Done JM, Holland GJ, Bruyère CL, Leung LR, Suzuki-Parker A (2012) Modeling high-impact weather and climate: lessons from a tropical cyclone perspective. NCAR Technical Note NCAR/TN-490 + STR. doi:10.5065/D61834FM
- Done JM, Holland GJ, Bruyère CL, Leung LR, Suzuki-Parker A (2013) Modeling high-impact weather and climate: lessons from a tropical cyclone perspective. *Clim Change*. doi:10.1007/s10584-013-0954-6
- Falk M, Pyles RD, Ustin SL, Paw UKT, Xu L, Whiting ML, Sanden BL, Brown PH (2013) Evaluated crop evapotranspiration over a region of irrigated orchards with the improved ACASA-WRF model. *J Hydrometeorol*. doi:10.1175/JHM-D-12-0183.1
- Gentry MS, Lackmann GM (2010) Sensitivity of simulated tropical cyclone structure and intensity to horizontal resolution. *Mon Wea Rev* 138:688–704
- Guo R-F, Xiao Z-N, Li Y, Shi W-J (2012) The statistical characteristics of impact of the westward-going tropical cyclones on rainfall in Yunnan Plateau. *J Trop Meteorol* 18(1):81–88
- Harr PA, Elsberry RL (1991) Tropical cyclone track characteristics as a function of large-scale circulation anomalies. *Mon Wea Rev* 119:1448–1468
- Hart RE (2003) A cyclone phase space derived from thermal wind and thermal asymmetry. *Mon Wea Rev* 131:585–616
- Holland GJ, Bruyère CL (2013) Recent intense hurricane response to global climate change. *Clim Dyn*. doi:10.1007/s00382-013-1713-0
- Hong S-Y, Lim J-OJ (2006) The WRF single-moment 6-class microphysics scheme (WSM6). *J Korean Meteorol Soc* 42:129–151
- Hong S-Y, Dudhia J, Chen S-H (2004) A revised approach to ice microphysical processes for the bulk parameterization of clouds and precipitation. *Mon Wea Rev* 132:103–120
- Huffman GJ, Adler RF, Bolvin DT, Gu G, Nelkin EJ, Bowman KP, Stocker EF, Wolff DB (2007) The TRMM multi-satellite precipitation analysis: quasi-global, multi-year, combined-sensor precipitation estimates at fine scale. *J Hydrometeorol* 8:33–55
- Janjic ZI (2000) Comments on “development and evaluation of a convection scheme for use in climate models”. *J Atmos Sci* 57:3686
- Kain JS (2004) The Kain–Fritsch convective parameterization: an update. *J Appl Meteorol* 43:170–181
- Kalnay et al (1996) The NCEP/NCAR 40-year reanalysis project. *Bull Am Meteorol Soc* 77:437–470. <http://www.esrl.noaa.gov/psd/data/gridded/data.ncep.reanalysis.derived.html>

- Kim H-J, Wang B (2011) Sensitivity of the WRF model simulation of the East Asian summer monsoon in 1993 to shortwave radiation schemes and ozone absorption. *Asia-Pac J Atmos Sci* 47(2):167–180
- Knapp KR, Kruk MC, Levinson DH, Diamond HJ, Neumann CJ (2010) The international best track archive for climate stewardship (IBTrACS): unifying tropical cyclone best track data. *Bull Am Meteorol Soc* 91:363–376
- Knutson TR, McBride JL, Chan J, Emanuel K, Holland G, Landsea C, Held I, Kossin JP, Srivastava AK, Sugi M (2010) Tropical cyclones and climate change. *Nat Geosci* 3. doi:10.1038/geo779
- Liang X-Z, Li L, Kunkel KE, Ting M, Wang JXL (2004) Regional climate model simulation of U.S. Precipitation during 1982–2002. Part I: annual cycle. *J Clim* 17:3510–3529
- Lin Y-L, Farley RD, Orville HD (1983) Bulk parameterization of the snow field in a cloud model. *J Clim Appl Meteorol* 22:1065–1092
- Ma ZH, Fei JF, Huang XG, Cheng XP (2012) Sensitivity of tropical cyclone intensity and structure to vertical resolution in WRF. *Asia-Pac J Atmos Sci* 48(1):67–81. doi:10.1007/s13143-012-0007-5
- PaiMazumder D, Done J (2013) Representation of temperature and precipitation extreme statistics in regional climate models. AOGS 2013, Brisbane, Australia, 22–28 June
- Raktham C, Kreasuwun J, Promnopas W (2007) Atmospheric dynamics of the tropical storm Vicente. *Chiang Mai J Sci* 34(2):171–182
- Ramage CS (1971) *Monsoon meteorology*. Academic Press, New York
- Raymond DJ (1995) Regulation of moist convection over the west Pacific warm pool. *J Atmos Sci* 52:3945–3959
- Reynolds RW (1988) A real-time global sea surface temperature analysis. *J Clim* 1:75–86
- Reynolds RW, Marsico DC (1993) An improved real-time global sea surface temperature analysis. *J Clim* 6:114–119
- Rosenthal SL (1971) The response of a tropical cyclone model to variations in boundary layer parameters, initial conditions, lateral boundary conditions, and domain size. *Mon Wea Rev* 99:767–777
- Shan H, Guan Y, Huang J (2012) Effects of spectral nudging on the 2010 East Asia summer monsoon using WRF model. *Chin J Oceanol Limnol* 30(6):1105–1115
- Shibin X, Bin W (2013) Enhanced western North Pacific tropical cyclone activity in May in recent years. *Clim Dyn*. doi:10.1007/s00382-013-1921-7
- Skamarock WC, Klemp JB, Dudhia J, Gill DO, Barker DM, Duda MG, Huang XY, Wang W, Powers JG (2008) A description of the advanced research WRF version 3. NCAR technical note TN-475 + STR
- Solomon S, Qin D, Manning M, Chen Z, Marquis M, Averyt K, Tignor MMB, Miller HL (eds) (2007) *Contribution of Working Group I to the 4th assessment report of the intergovernmental panel on climate change*. Cambridge University Press, Cambridge, United Kingdom, and New York, NY, USA
- Stowasser M, Wang Y, Hamilton K (2007) Tropical cyclone changes in the Western North Pacific in a global warming scenario. *J Clim* 20:2378–2396
- Suzuki-Parker A (2012) *An assessment of uncertainties and limitations in simulating tropical cyclones*. Springer, Thesis XIII, 78 pp
- Tao SY, Chen LX (1987) A review of recent research on the East Asia summer monsoon in China. In: Chang CP, Krishnamurti TN (eds) *Monsoon meteorology*. Oxford University Press, Oxford, pp 60–92
- Tao W-K, Shi JJ, Chen SS, Lang S, Lin P-L, Hong S-Y, Peters-Lidard C, Hou A (2011) The impact of microphysical schemes on hurricane intensity and track. *Asia-Pac J Atmos Sci* 47(1):1–16
- Thailand Cabinet Resolution (2005) <http://www.eppo.go.th/admin/cab/cab-2548-09-20.html>
- Thompson G, Rasmussen RM, Manning K (2004) Explicit forecasts of winter precipitation using an improved bulk microphysics scheme. Part I: description and sensitivity analysis. *Mon Wea Rev* 132:519–542
- Wang B, Lin H (2002) Rainy season of the Asian–pacific summer monsoon. *J Clim* 15:386–398
- Wangwongchai A, Zhao SX, Zeng QC (2010) An analysis of Typhoon Chanthu in June 2004 with focus on the impact on Thailand. *Adv Atmos Sci* 27(1):14–32
- Webster PJ, Holland GJ, Curry JA, Chang H-R (2005) Changes in tropical cyclone number, duration, and intensity in a warming environment. *Science* 309:1844–1846
- Wei W, Zhang R, Wen M, Rong X, Li T (2013) Impact of Indian summer monsoon on the South Asian High and its influence on summer rainfall over China. *Clim Dyn*. doi:10.1007/s00382-013-1938-y
- Ying M, Knutson TR, Kamahori H, Lee T-C (2012) Impacts of climate change on tropical cyclones in the Western North Pacific Basin. Part II: late twenty-first century projections. *Trop Cyclone Res Rev* 1(2):231–241
- Yun KS, Chan JCL, Ha KJ (2012) Effects of SST magnitude and gradient on typhoon tracks around East Asia: a case study for Typhoon Maemi (2003). *Atmos Res* 109–110:36–51